Available online at www.sciencedirect.com
ScienceDirect
Journal of the European Ceramic Society 32 (2012) 227–234
www.elsevier.com/locate/jeurceramsoc

Microstructure of Fe–$ZrSiO_4$ solid solutions prepared from gels

G. Herrera, N. Montoya, J. Alarcón *

Department of Inorganic Chemistry, University of Valencia, Calle Dr. Moliner 50, 46100 Burjasot, Valencia, Spain

Received 29 April 2011; received in revised form 27 July 2011; accepted 6 August 2011
Available online 30 August 2011

Abstract

Microstructural changes associated with chemical and structural evolution from gels to Fe_x–$ZrSiO_4$ solid solutions are reported. Mineralizer-free Fe_x–$ZrSiO_4$ gels in the compositional range $0 \leq x \leq 0.15$ were prepared by sol–gel liquid-phase route from mixtures of alkoxides of silicon and zirconium, and iron (III) acetylacetonate, and annealed at different temperatures and/or times.

The first step on the whole process to the final Fe_x–$ZrSiO_4$ solid solutions was the formation of aggregated of tetragonal Fe-doped ZrO_2 nanocrystals with diameters smaller than 50 nm. At this stage the tetragonal Fe–ZrO_2 were embedded in amorphous silica resulting nanocomposite materials. The formation of the final Fe_x–$ZrSiO_4$ solid solution nanocrystals at around 1100 °C occurred almost simultaneously to the Fe–ZrO_2 solid solution phase transformation from the tetragonal to the monoclinic form. The microstructural examination of specimens after annealing at 1200 °C revealed the development of Fe-doped zircon nanoparticles smaller than 100 nm.

Keywords: Powders-chemical preparation; Sol–gel processes; Microstructure; Traditional ceramics; Fe–$ZrSiO_4$

1. Introduction

The coral iron–zircon is one of the three classical zircon-based ceramic pigments. Since its discovery in the 60s, it has been one of the most widely used reddish colours in the ceramic industry.[1,2] However, the nature of this pigmenting ceramic system remains controversial. While it is considered by some authors as to be formed by particles of hematite encapsulated in a zircon matrix, other researchers state that also an important component of that pigment is the solid solution formed by the entry of Fe cations into the zircon structure.[3–7] There is an interest, therefore, to clarify different fundamental aspects of this ceramic pigment, mainly the ones regarding with that solid solution and particularly the distribution and amount of Fe cations in the zircon structure. Of course, is also interesting to evaluate whether particulated Fe-containing zircon materials develop enough tinctorial strength to achieve the requirements for this ceramic pigment system.

Ceramic pigments are particulated ceramic materials used as dispersed particles in industrial applications. Although the developed microstructure influences the optical properties of these particulated ceramic materials, as far as we know it has not been a subject of extended study. Some parameters such as the size and shape of non-aggregated particles are very important in these ceramic applications. Nowadays, these characteristics reach even more importance because of the modern ways of colour application used in industrial processes, such as the inkjet-printing, nanometric non-aggregated pigmenting particles are required.

Different chemical techniques of preparation of powdered solids have been used during the last decade, mainly with the purpose of controlling both the shape and the size of non-aggregated particles. In some cases, the powdered solids were obtained as amorphous, so that it was required some specific thermal treatment to develop the desired crystalline form.The preparation of particulate either pure or doped zircon have received some attention in the last decade. However, some reports on zircon-derived materials prepared by different techniques concluded with the formation of aggregated particles.[4,6–8]

Some years ago we assessed the use of sol–gel liquid-phase routes to control the size and shape of particles in vanadium-doped zircon solid solutions.[9] Interestingly, even at relatively high temperature, i.e. 1100 °C, it was possible to obtain almost non-aggregated particles. These findings opened new chances and the possibility to control the shape and size of final particles in other zircon-based ceramic pigmenting systems.

* Corresponding author. Tel.: +34 96 3544584; fax: +34 96 3544322.
E-mail address: javier.alarcon@uv.es (J. Alarcón).

0955-2219/$ – see front matter © 2011 Elsevier Ltd. All rights reserved.
doi:10.1016/j.jeurceramsoc.2011.08.014

The main goal of this work is the preparation of final non-aggregated particles of Fe–zircon solid solutions by sol–gel techniques. Also, we intend to examine the microstructural changes coupled to the chemical and structural transformations on annealing from gels to final zircon solid solutions. The microstructural features of tetragonal Fe–ZrO_2–amorphous silica particulate composite materials obtained through the process leading to the final Fe–zircon from gels are also studied.

2. Experimental procedure

2.1. Preparation of samples

Gels with stoichiometry, Fe_x–$ZrSiO_4$, in the range of compositions $0 \leq x \leq 0.125$, were prepared by the sol–gel liquid-phase route, using zirconium n-propoxide (ZnP, $Zr(OC_3H_7)_4$), tetraethylorthosilicate (TEOS, $Si(OC_2H_5)_4$) and iron acetylacetonate ($Fe(acac)_3$, $FeC_{15}H_{24}O_6$), as sources for Zr, Si and Fe, respectively. Acetylacetone (acac, $C_5H_8O_2$) and 1-propanol (n-PrOH) were used as chelating agent and solvent, respectively. There are two main steps in the preparation of gel precursors. Firstly, the stoichiometric amounts of the different reagents are dissolved in ETOH. The second step involves the formation of a colloidal solution from the prior solution and its subsequent gelling. Thus, the synthetic procedure was as follows. At the beginning the stoichiometric contents of ZnP and $Fe(acac)_3$ were added to a mixture of PrOH and acac. The main goal at this stage is to prevent the formation of precipitates by fast hydrolysis of the alkoxides, mainly the zirconium one. Then, the required amounts of TEOS and H_2O were added to the mixture to obtain the resulting solution leading to the gel. Subsequently, the resulting solution maintained in a closed polyethylene bottle at 60 °C for 24 h yielded the final gel. The ZnP:n-PrOH:acac:TEOS:H_2O molar ratios used in the preparation of this series of samples were 1:8:1:1:5.5.

The final gels dried at 120 °C were annealed at different temperatures from 400 °C to 1600 °C during different times.

2.2. Techniques of characterization

Different techniques were used to follow the chemical and structural changes, and the coupled microstructural evolution.

Infrared absorption spectra (Model 320, Avatar, Nicolet) were carried out in the range 2000–400 cm^{-1} using the KBr pellet method.

X-ray diffraction analysis (Model AXS D5005 Bruker) was performed using a graphite monochromatic CuK_α radiation. The diffractograms were run with a step size of 0.02° 2θ and a counting time of 10 s. The microstructure of the as-prepared and thermally treated samples was determined by field emission scanning electron microscopy at 20–30 kV (Model S-4100, Hitachi Ltd., Tokyo, Japan). Samples were etched with a diluted 30% (v/v) HF solution for times between 20 and 30 s, and subsequently washed with H_2O, to improve the observation. All specimens were coated with gold/palladium in an ion beam coater.

The morphology of iron-containing zirconia and zircon particles was also examined using transmission electron microscopy (Model 1010, Jeol Ltd., Tokyo, Japan) at an accelerating voltage of 100 kV. Samples were crushed and dispersed in absolute ethyl alcohol and drops of the dispersion were transferred to a specimen copper grid carrying a lacey carbon film. Particle size analyses were carried out by using the ImageJ software.

Energy-dispersive X-ray analysis was performed using a scanning electron microscope (Model XL30, ESEM, Philips) operated at 20 kV. This instrument is equipped with an energy dispersive X-ray spectrometer (Model XL30 132-2.5, EDAX). Two kind of analysis were carried out in order to obtain either the overall chemical composition of samples or the chemical composition of specific crystalline phases. The first one was performed by the area mode and at relatively low magnification while the second by the spot mode stopping the electron beam on the point to be analyzed. Quantitative analyses of specimens were obtained using the EDAX-GENESIS program with ZAF correction procedures and the default standards.

L^* a^* b^* parameters of specimens were obtained using a spectrophotometer (Model UV670-670, Jasco) using a standard lighting C, following the CIE-L^* a^* b^* colorimetric method recommended by the CIE (Commision Internationale de l'Eclairage). In this colour system, L^* is the colour lightness ($L^* = 0$ for black and 100 for white), a^* is the green (−)/red (+) axis, and b^* is blue (−)/yellow (+) axis.

3. Results and discussion

3.1. Infrared spectroscopy of dried and annealed gels

The structural and chemical evolution of gels will be determined by the chemical homogeneity reached in their preparation. In general, the changes will be dependent on the polymeric or colloidal nature of gels. In the former ones a single phase gel is formed while in the later a complete chemical homogeneity is not attained and a multiphasic system is developed, i.e. particles with domains with different chemical nature. IR spectra of dried and annealed gels $Fe_{0.02}$–$ZrSiO_4$ at different temperatures are shown in Fig. 1. As can be seen dried gels display bands at around 1023 and 470 cm^{-1}. The first one can be associated with the stretching mode of the Si–O bond[10] while the second can be attributed to both the bending mode of the O–Si–O bond and the stretching mode of the Zr–O bond.[10,11] On heating at 1000 °C a strong change is observed in the IR spectra of the annealed gel. Thus, a band appears at 586 cm^{-1}, which can be attributed to the presence of crystallized zirconia in the tetragonal form.[11] In addition, peaks detected at 800 cm^{-1} can be ascribed to the bending modes of Si–O–Si bond. Also a shoulder at 1204 cm^{-1} is detected in the spectra that can also be assigned to the Si–O–Si asymmetric bond stretching vibrations.[9,12,13] At this stage after annealing at 1000 °C, it can be assumed the segregation of silica, as suggested by the shift of the stretching mode of the Si–O bond to higher wave number, around 1086 cm^{-1}.[10] Therefore, the gel precursors can be considered at least as diphasic, i.e. a phase based on zirconia and other based on amorphous silica. IR spectra of gels annealed at 1100 °C and 1200 °C are very sim-

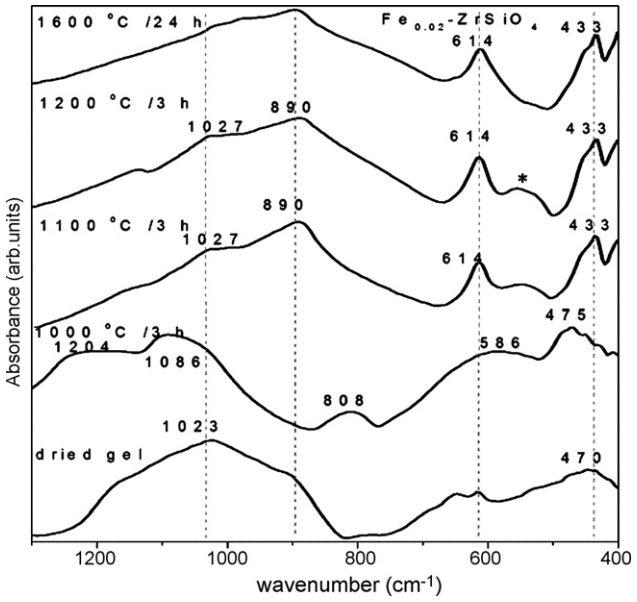

Fig. 1. IR spectra of $Fe_{0.02}$–$ZrSiO_4$ dried gel and after annealed at different temperatures.

Table 1
Average chemical composition (wt.% in oxides) of major crystalline phases at different stages through the zircon after annealing gels at different temperatures.

Sample	T (°C)	SiO_2	ZrO_2	Fe_2O_3
$x = 0.02$	Dried gel	35.9(2)	62.6(3)	1.5(2)
	1000/3 h	–	98.0(5)	2.0(5)
	1200/3 h	37.0(3)	61.7(4)	1.4(2)
	1600/24 h	37.5(3)	61.5(4)	1.0(1)
$x = 0.05$	Dried gel	37.0(4)	60.4(3)	2.6(2)
	1000/3 h	–	96.0(2)	4.0(2)
	1100/3 h	34.7(5)	61.9(5)	3.4(5)
	1600/24 h	35.8(5)	60.9(5)	3.3(4)
$x = 0.07$	Dried gel	35.8(1)	59.8(2)	4.6(3)
	1000/3 h	–	93.2(5)	6.8(5)
	1100/3 h	33.2(5)	61.9(5)	5.0(5)
	1600/24 h	37.1(4)	60.7(3)	2.2(2)
$x = 0.1$	Dried gel	35.5(2)	58.8(2)	5.7(2)
	1000/3 h	–	89.5 (5)	10.5(5)
	1100/3 h	35.9(4)	58.1(4)	6.1(5)
	1600/24 h	31.5(5)	63.7(5)	4.8(5)

ilar, displaying bands at 1027, 890, 614 and 433 cm^{-1} which correspond to the formation of a crystalline phase with zircon structure.[14]

3.2. Structural and compositional evolution of gels through the thermal treatment

In this point we will follow the transformations occurred in gels over the range of temperature between 400 °C and 1600 °C, i.e. from dried gels to the formation of phases with zircon structure in the range 1100–1200 °C, and at higher temperatures to check their stability. It is intended to determine not only the structure of the developed crystalline phases on increasing the annealing temperature but also the temperature range at which they are metastable and their average composition.

As a reference for comparing the structural evolution of doped gels it is valuable to consider the structural evolution of the undoped gel, i.e. $ZrSiO_4$, prepared by the synthetic procedure used for the Fe-doped ones. It is to note that the transformations leading to zircon from undoped gels are quite similar to the ones reported in a previous paper regarding with zircon formation on annealing gel precursors but prepared by gelling mixtures of previously prepared ZrO_2 nanoparticles and TEOS.[15] In summary, on heating the undoped gel at around 800 °C appears a set of broad peaks which can be associated with a phase with tetragonal zirconia structure. The intensity of the XRD peaks increases after annealing for short time at 1200 °C. Before the formation of the zircon phase the tetragonal to monoclinic phase transformation of zirconia takes place. That transformation is detected on annealing gels at 1400 °C for short time. On longer annealing at 1400 °C pure zircon is completely developed. These results are in agreement with ones previously reported on zircon formation using different synthetic procedure.[8,15,16] It is to be noted that the undoped gel precursor in the present work was prepared by controlled hydrolysis and condensation of a solution mixture of ZnP and TEOS. That one-step process leads to a dried gel made up of small aggregates of inorganic–inorganic nanocomposites of silica-coated zirconia nanoparticles. The factors governing the reaction sequence leading to pure zircon formation and the critical phase transformation from tetragonal to monoclinic ZrO_2 in our undoped gel precursor can been understood by considering some facts already reported in the literature.[17–19] From the above results can be concluded that there are no significant differences in the structural evolution to zircon from either the gel obtained by gelling mixtures of previously prepared colloidal ZrO_2 particles and TEOS[15] or the one obtained by one-step gelling mixtures of silicon and zirconium alkoxides.

Regarding the effect of the iron dopant on the temperature of zircon solid solution formation, it is evidenced by X-ray diffraction that for gels with a relatively small content of iron, i.e. $Fe_{0.02}$–$ZrSiO_4$, the required temperature for full development of phase with zircon structure lowers significantly. In Figs. 2–5 are shown the XRD patterns of gels $Fe_{0.02}$–$ZrSiO_4$, $Fe_{0.05}$–$ZrSiO_4$, $Fe_{0.07}$–$ZrSiO_4$ and $Fe_{0.1}$–$ZrSiO_4$, respectively. The diffractograms for gels with $x = 0.02$ annealed at 1200 °C and for the rest of gels annealed at 1100 °C, display patterns characteristic of a phase with zircon structure. However, it is to be noted that for the gel with the larger nominal amount of iron ($x = 0.1$) a relatively large amount of a secondary phase with structure of tetragonal zirconia as well as some peaks corresponding to hematite are also detected at 1100 °C. After annealing gels at higher temperatures than 1200 °C, at which the Fe–zircon phase is fully developed as can be seen for the corresponding XRD patterns, there are no appreciable structural changes.

The compositional variation in zircon particles after annealing at temperatures higher than the lowest ones required to developing iron–zircon solid solution as single phase is quite interesting. EDX/SEM microanalysis measurements carried out from gels annealed at 1200 °C for 3 h and 1600 °C for 24 h are shown in Table 1. It is to note that these measurements were per-

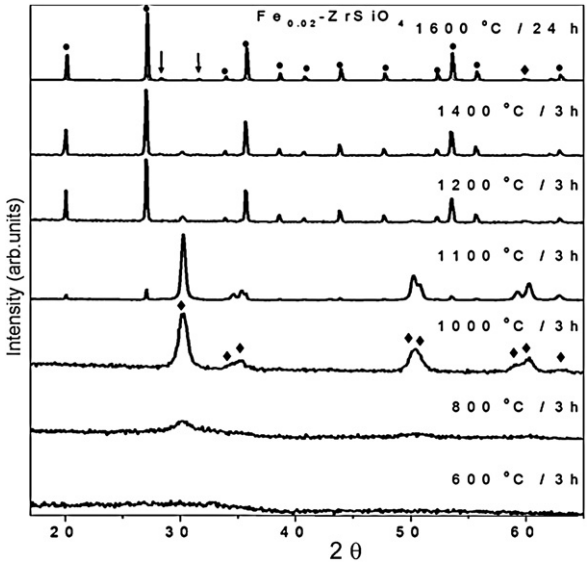

Fig. 2. XRD patterns of specimen $Fe_{0.02}$–$ZrSiO_4$ on annealing at different temperatures up to 1600 °C. (♦) Tetragonal ZrO_2, (↓) monoclinic, and (●) zircon.

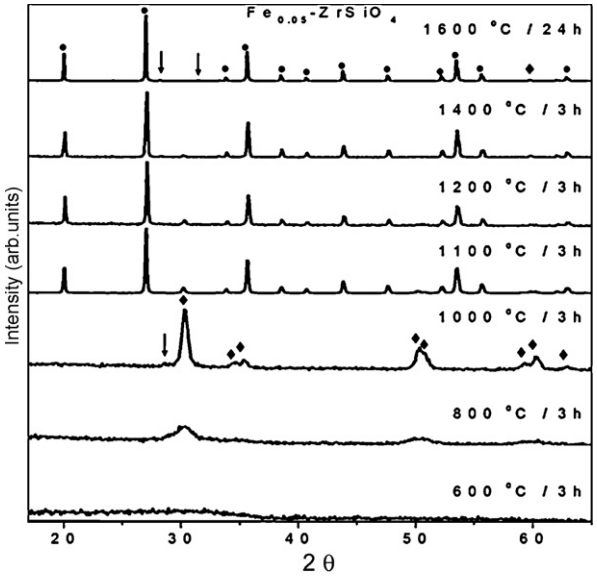

Fig. 3. XRD patterns of specimen $Fe_{0.05}$–$ZrSiO_4$ on annealing at different temperatures up to 1600 °C. (♦) Tetragonal ZrO_2, (↓) monoclinic, and (●) zircon.

formed on etched specimens with HF acid solution in order to remove the small portion of amorphous silica still present after annealing. In general, it can be observed that with the method and procedures used in the quantitative determination, the amounts of Fe_2O_3 are a little bit overestimated in all dried gel precursors. However, from these results an evaluation of the iron content inside the zircon phase may be done. As can be seen the obtained contents of iron (as Fe_2O_3 wt.%) in the zircon phase on annealing at 1100 °C (or 1200 °C) are very close to the nominal ones for all the different compositions. This result means that most of the nominal iron is into the zircon phase in the sample series. However, for the specimens with high Fe contents, $Fe_{0.07}$–$ZrSiO_4$ and $Fe_{0.1}$–$ZrSiO_4$, long annealed at the higher temperature, i.e. for 24 h at 1600 °C, the amount of Fe significantly decreases. This decreasing in the content of Fe into the zircon host lattice can be caused by the instability of the Fe–zircon solid solution at higher temperatures than 1200 °C. However, the iron exsolved from the zircon phase is almost undetected in the XRD patterns as crystalline hematite phase. The most part of that iron oxide, therefore, could be solved in the small amount of amorphous silica still remaining in the specimens.

From the above coupled XRD and EDX results it can be drawn that almost all the nominal iron is dissolved into the zircon structure in Fe-containing zircon (Fe_x–$ZrSiO_4$) gels up to $x = 0.07$ annealed at 1100 °C (1200 °C for $x = 0.02$), whereas for gels with higher nominal amounts of Fe ($x \geq 0.7$) a small portion of Fe is crystallized as hematite. It is also noted that is not detected hematite as secondary crystalline phase on annealing gels with $x \leq 0.07$ at the highest temperature, i.e. at 1600 °C for 24 h, even though the amounts of solved Fe into the zircon phases decrease (Table 1).

As can be seen in Figs. 2–5 the first step in the whole process leading to Fe–zircon for all the annealed gels is the formation of a crystalline phase with the structure of tetragonal zirconia. These crystalline phases are detected by XRD of specimens annealed at around 800 °C and fully developed at 1000 °C. There are no large differences in the stability range of these zirconia-based tetragonal crystalline phases for the specimens with different nominal amount of Fe. The composition of these tetragonal Fe–ZrO_2 solid solutions in the series of gels Fe_x–$ZrSiO_4$ annealed at 1000 °C for 3 h is also shown in Table 1. EDX microanalysis was performed after etching with a HF acid solution to remove the silica component. As can be seen the amount of Fe inside the tetragonal ZrO_2 phase is raised on increasing the nominal amount of Fe in the series of samples. This trend indicates that the amount of iron that can be dissolved into the tetragonal zirconia lattice will be higher than 6 wt.% of Fe_2O_3 (corresponding to the stoichiometry $Fe_{0.1}$–ZrO_2). As far as we know there is no information in the literature about the limit of solubility of Fe in

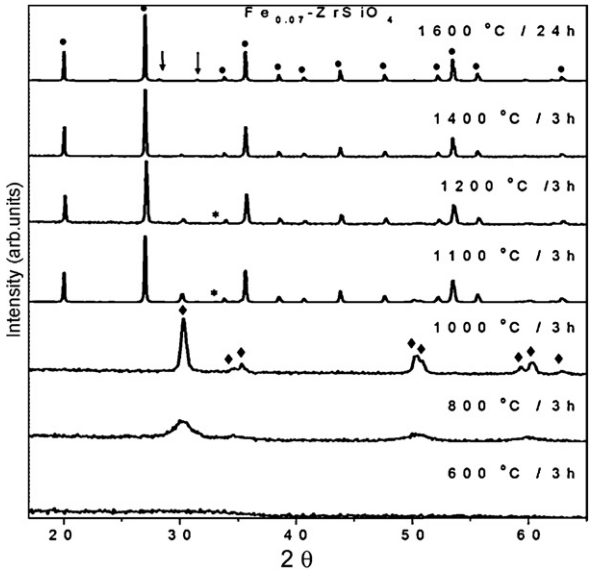

Fig. 4. XRD patterns of specimen $Fe_{0.07}$–$ZrSiO_4$ on annealing at different temperatures up to 1600 °C. (♦) Tetragonal ZrO_2, (↓) monoclinic, (●) zircon, and (*) hematite.

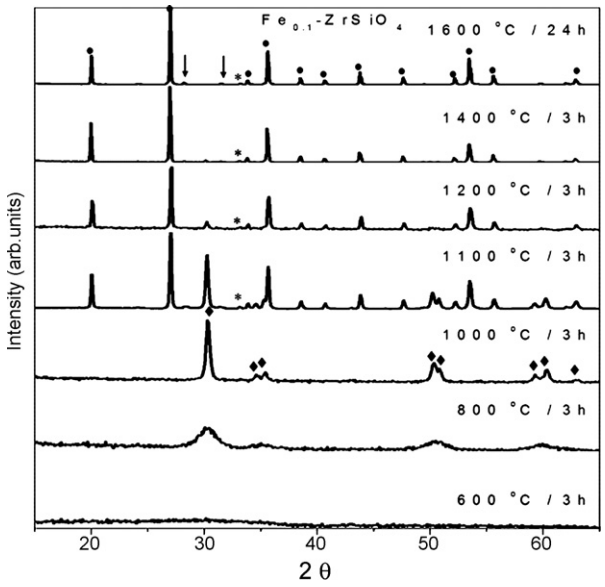

Fig. 5. XRD patterns of specimen $Fe_{0.1}$–$ZrSiO_4$ on annealing at different temperatures up to 1600 °C. (♦) Tetragonal ZrO_2, (↓) monoclinic, (●) zircon, and (*) hematite.

tetragonal ZrO_2. We are currently studying the binary system in order to determine structural parameters of these solid solutions in the Fe_2O_3–ZrO_2 binary system.

Obviously, as evidenced by IR spectroscopy and confirmed by the fact that no silicon-based crystalline phase is detected by XRD, the silicon component must be as amorphous silica at this first stage in the annealing of gels. However the striking fact is that the tetragonal to monoclinic transformation of Fe–ZrO_2 phases in the different annealed gels is almost undetected by XRD. It obviously happens, but almost simultaneously takes place the reaction with the amorphous silica to produce zircon. In the XRD patterns of gels annealed at around 1100 °C in Figs. 2–5, peaks of the monoclinic form of ZrO_2 are, in fact, very weak. Thus the development of Fe–zircon phases from gels is speeded at as low annealing temperature as 1100 °C.

It seems worthwhile some comments on the differences in the kinetic of formation of different M-containing zircon solid solutions from gels. In the V–$ZrSiO_4$ case has been proved that the V itself catalyze the reaction of zircon phase formation, in such a way that on increasing the amount of nominal vanadium the temperature of zircon formation decreases.[9,15] Our results on Fe–$ZrSiO_4$ indicate also a role of catalyser for Fe, but for this system the temperature for full development of the Fe–zircon phase reaches a minimum for nominal contents of iron in the starting precursor in the range $0.02 \leq x \leq 0.05$. It is to note that the temperature of complete development of Fe–zircon phases does not change with higher contents of iron in the gel precursor. Anyway, the temperatures of formation of V– and Fe–zircon solid solutions from free-mineralizer gel precursors are relatively low in both cases. This similar behaviour in the whole process of V– and Fe–$ZrSiO_4$ solid solutions formation can be understood by certain parallelism in the stability of both monoclinic V- and Fe-containing ZrO_2 solid solutions. For the V–$ZrSiO_4$ was reported that on increasing the vanadium content the tetragonal to monoclinic transformation of V–ZrO_2 occur at lower temperatures and the subsequent reaction with silica occurs almost immediately after the formation of the monoclinic form.[9,13] For the Fe–$ZrSiO_4$ we have seen that in the series of samples the formation of the tetragonal crystalline form of the Fe-containing ZrO_2 occurs at similar temperatures, and their transformation temperature to the monoclinic form does not depend on the iron nominal content but occurred at around 1100 °C for all samples. As far as we know there are no reported accurate information on the preparation and stability of tetragonal and monoclinic Fe–ZrO_2 solid solutions in the Fe_2O_3–ZrO_2 binary system. The instability of these monoclinic M–ZrO_2 (M = V, Fe) solid solutions could be mainly attributed to the different ionic sizes of Fe^{3+}, V^{4+} and Zr^{4+} cations.[20]

3.3. Microstructural changes from gels to Fe–$ZrSiO_4$ particles

As inferred from XRD, IR and EDX results the whole process of Fe–zircon formation from annealed gel precursors at different temperatures occurs through three steps. Although three different types of crystalline phases are detected, only two can be fully developed over the annealing of gels. The tetragonal Fe_x–ZrO_2 formed at the crystallization beginning from gels and the final Fe_x–$ZrSiO_4$ phase. The second structural change leading to monoclinic Fe_x–ZrO_2 is sometimes even very difficult to detect. This behaviour suggests that simultaneously to the tetragonal to monoclinic zirconia phase transformation the reaction between the monoclinic Fe–zirconia and the amorphous silica to form Fe–zircon takes place.

In order to take a more complete picture of the reactivity from the gel precursors to the zircon phases, it is worthwhile to relate the structural changes to the microstructural transformations. Thus, the microstructural evolution of samples $Fe_{0.02}$–$ZrSiO_4$ and $Fe_{0.1}$–$ZrSiO_4$, annealed at the required temperatures to which the tetragonal Fe_x–ZrO_2 and the final Fe_x–$ZrSiO_4$ are fully developed, is examined by FESEM and TEM. In Fig. 6 are shown FESEM micrographs of gels $Fe_{0.02}$–$ZrSiO_4$ (Fig. 6a) and $Fe_{0.1}$–$ZrSiO_4$ (Fig. 6b) annealed at 1050 °C and 1100 °C for 3 h, respectively, after etching with HF acid solution for removing the amorphous silica phase. For both compositions can be distinguished quasi-spherical particle aggregates, with diameters much lower than 50 nm. TEM micrographs of these as-prepared samples, i.e. without any etching to remove the amorphous silica are shown in Fig. 7. Interestingly, it can be observed that at this stage the non-aggregated smaller particles are made up by two components with different contrast. In fact they are nanocomposite particles in which the tetragonal Fe–ZrO_2 core is coated with an outer layer of amorphous silica. In both specimens the average size of these inorganic–inorganic core–shell nanocomposite particles is around 10 nm.

On increasing the annealing temperature to 1200 °C for both specimens $Fe_{0.02}$–$ZrSiO_4$ and $Fe_{0.1}$–$ZrSiO_4$, the final phase with zircon structure is fully developed. The microstructure of these specimens prepared on annealing at 1200 °C for 3 h are displayed in Fig. 8. As can be seen an arrangement of particles with sizes around 100 nm is observed. It seems that the amount

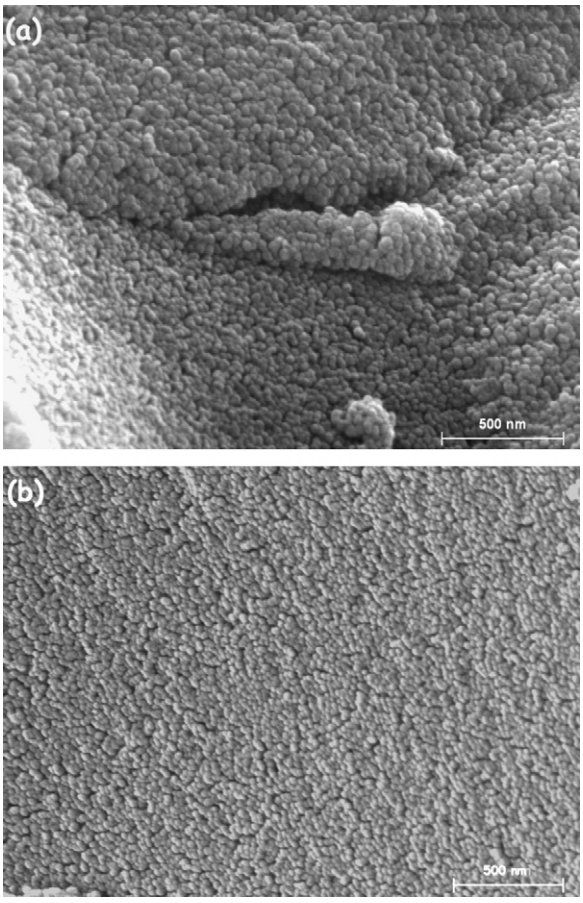

Fig. 6. FESEM micrographs of dried gels annealed at different temperatures yielding tetragonal Fe–ZrO_2 as single crystalline phase: (a) $Fe_{0.02}$–$ZrSiO_4$ at 1050 °C for 3 h and (b) $Fe_{0.1}$–$ZrSiO_4$ at 1100 °C for 3 h.

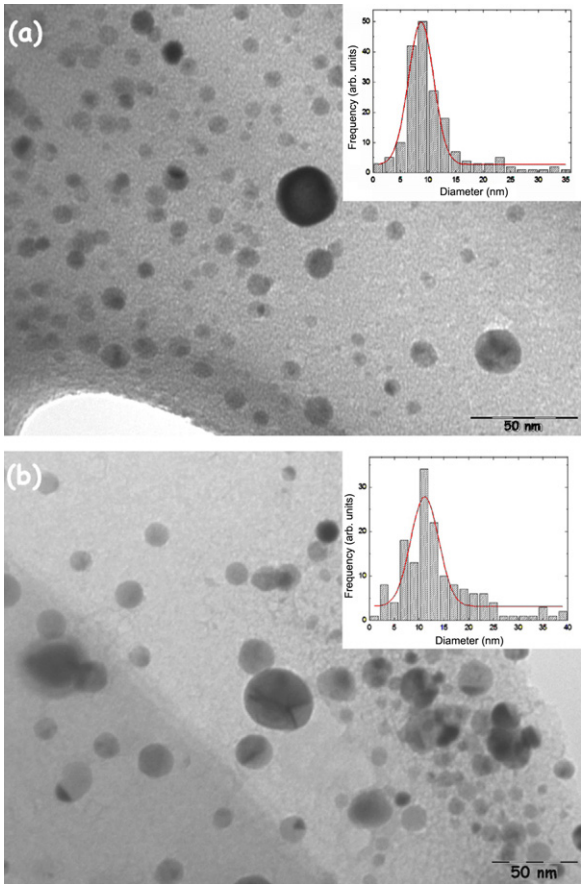

Fig. 7. TEM micrographs of dried gels annealed at different temperatures yielding tetragonal Fe–ZrO_2 as single crystalline phase: (a) $Fe_{0.02}$–$ZrSiO_4$ at 1050 °C for 3 h and (b) $Fe_{0.1}$–$ZrSiO_4$ at 1100 °C for 3 h.

of dopant does not influence the size of Fe–$ZrSiO_4$ nanoparticles. The composition of the Fe_x–$ZrSiO_4$ solid solutions in the series of gels annealed at 1100 (or 1200) °C for 3 h is also shown in Table 1. As mentioned above, EDX microanalyses were performed after etching with diluted HF acid solution to remove the small amount of amorphous silica coating the Fe–zircon particles. For the specimen with nominal composition $Fe_{0.1}$–$ZrSiO_4$ the amount of iron as Fe_2O_3 wt.% is 6.1, which must be a bit overestimated. Taking into account the detection of hematite by XRD in this sample, it can be drawn that the solubility of iron oxide in zircon is over 0.07 mol of Fe_2O_3 per mol of zircon. It is interesting to mention that an increase on annealing temperature give rise to an increase of zircon particle size. Thus, gels of the above mentioned compositions annealed at 1600 °C for 24 h reach sizes about 5 μm. As can be seen in Table 1 the amount of iron at this high temperature decrease for all samples. This fact can be due to the instability of the Fe–$ZrSiO_4$ solid solutions at so high temperatures, decreasing the amount of Fe dissolved in the $ZrSiO_4$ lattice. Results from XRD patterns of the specimens annealed at that high temperature suggest that the most part of the removed Fe is dissolved into the small amount of amorphous silica.

There are certain similarities in the microstructural evolution leading to the formation of either M–$ZrSiO_4$ (M = Fe or V) solid solutions. In both types of solid solutions the three structural and microstructural steps are quite similar. Thus, through the thermal annealing at different temperatures and times, the gel precursors transform firstly in an arrangement of tetragonal M–ZrO_2–amorphous silica core–shell composed nanoparticles. On further annealing the crystalline core with tetragonal zirconia structure transforms to the monoclinic form. In both systems the stability of the monoclinic M–ZrO_2 is very low. Finally, by subsequent annealing the reaction between the silica coating and the monoclinic doped zirconia particle core takes place and doped zircon is formed. The main difference between both types of processes leading to M–$ZrSiO_4$ final products is mainly the strong catalyser effect of V in the zircon formation.

3.4. Colour in Fe–$ZrSiO_4$ solid solutions

L a* b** parameters have been obtained from the diffuse reflectance spectra. The obtained data as the nominal iron content increases in samples annealed at the lower temperature for complete zircon formation, i.e. 1100 °C and 1200 °C are reported in Table 2. Also, for the sake of comparison the colorimetric parameters of a commercial iron–zircon pigment, prepared by the conventional solid state reaction, are included.

As can be seen in all specimens the values of *a**, which is the parameter representative of the red colour, correspond to a

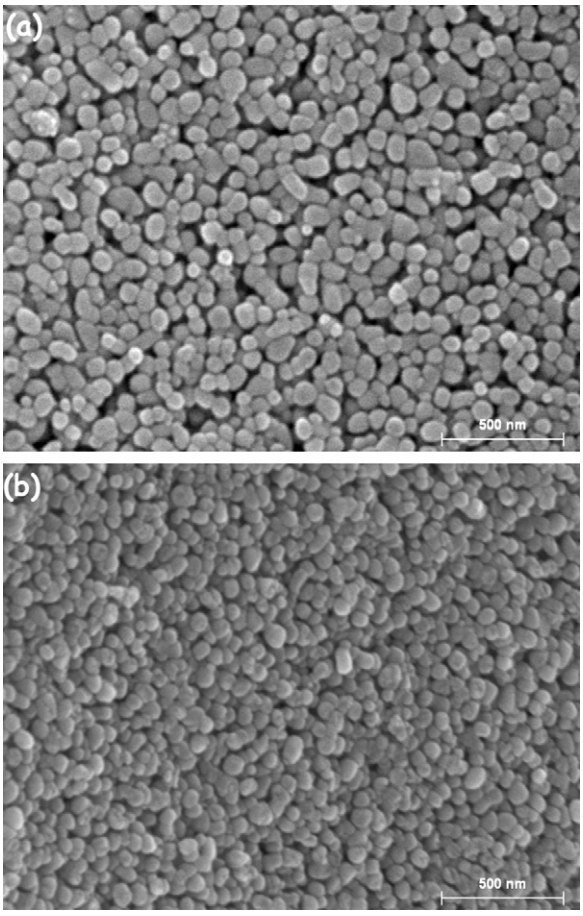

Fig. 8. FESEM micrographs of dried gels annealed at 1200 °C for 3 h: (a) $Fe_{0.02}$–$ZrSiO_4$ and (b) $Fe_{0.1}$–$ZrSiO_4$.

reddish tint. The trend of L^* and a^* parameters in the series of prepared Fe_x–$ZrSiO_4$ solid solutions shows that the L^* parameter decreases and the a^* parameter increases with the iron content up to the specimen $Fe_{0.07}$–$ZrSiO_4$, On increasing the nominal iron content these parameters almost remain constant. The $Fe_{0.07}$–$ZrSiO_4$ sample, therefore, shows the more intense coral hue with the smaller content of nominal iron.

In general, in the series of specimens Fe_x–$ZrSiO_4$ was not detected significant variation of a^* on heating a given sample at temperatures in the range between 1100 °C and 1300 °C. It is to note that the L^* and a^* parameters of sample $Fe_{0.07}$–$ZrSiO_4$ annealed at 1100 °C are comparable to those corresponding to a commercial iron–zircon pigment, although the former is a Fe–zircon solid solution prepared both with a low content of iron and mineralizer-free and the commercial one was elaborated with a large excess of iron and mineralizer.

Table 2
L^* a^* b* parameters of samples Fe_x–$ZrSiO_4$ annealed at 1100 °C and/or 1200 °C for 3 h.

Sample	T (°C)	L^*	a^*	b^*
Commercial iron–zircon	1200	40.63	16.43	8.56
$Fe_{0.02}$–$ZrSiO_4$	1200	65.78	12.29	17.07
$Fe_{0.07}$–$ZrSiO_4$	1100	48.94	28.04	27.74
$Fe_{0.1}$–$ZrSiO_4$	1100	46.58	28.30	27.70
$Fe_{0.1}$–$ZrSiO_4$	1200	45.18	27.58	26.04

4. Conclusions

Microstructural changes associated with chemical and structural evolution through the whole formation process of Fe–zircon solid solutions from gels are reported. Fe_x–$ZrSiO_4$ gels in the compositional range $0 \leq x \leq 0.15$ were prepared by sol–gel liquid-phase route from mixtures of alkoxides of silicon and zirconium, and iron (III) acetylacetonate. The chemical evolution and the crystallization pathway on annealing gels were followed by infrared (IR) and energy dispersive X-ray (EDX) spectroscopies, and X-ray diffraction (XRD) and the microstructural changes by scanning and transmission electron microscopy (SEM and TEM).

Results indicated the formation of tetragonal Fe-doped ZrO_2 nanocrystals as first step on the whole process to the final Fe_x–$ZrSiO_4$ solid solutions. The microstructure associated consisted of tetragonal Fe-doped ZrO_2–amorphous silica core–shell nanocomposites. The formation of the final Fe_x–$ZrSiO_4$ solid solution nanocrystals at around 1100 °C occurred almost simultaneously to the tetragonal to monoclinic phase transformation of Fe–ZrO_2 solid solutions. The microstructural examination of specimens after annealing at 1200 °C revealed the development of Fe-doped zircon nanoparticles with sizes around 100 nm.

Acknowledgments

G. Herrera thanks CONACyT for a postdoctoral fellowship Grant no. 129569. Financial support from the MICINN (Ministry of Science and Innovation) through the CONSOLIDER-INGENIO 2010 program to the project CDS2010-00065 is acknowledged.

References

1. Eppler RA. Zirconia-based colors for ceramic glazes. *Am Ceram Soc Bull* 1977;**56**:213–5, 218.
2. Eppler RA. Kinetics of formation of an iron–zircon pink color. *J Am Ceram Soc* 1977;**62**:47–9.
3. Berry FJ, Eadon D, Holloay J, Smart LE. Iron-doped zirconium silicate. Part 1. The location of iron. *J Mater Chem* 1996;**6**:221–5.
4. Tartaj P, González-Carreño T, Serna CJ, Ocaña M. Iron zircon pigments prepared by pyolysis of aerosols. *J Solid State Chem* 1997;**128**:102–8.
5. Cappelletti G, Ardizzone S, Fermo P, Gilardoni S. The influence of iron content on the promotion of the zircon structure and the optical properties of the pink coral pigments. *J Eur Ceram Soc* 2005;**25**:911–7.
6. Ardizzone S, Binaghi L, Cappelletti G, Fermo P, Gilardoni S. Iron doped zirconium silicate by a sol–gel procedure. The effect of the reaction conditions on the structure, morphology and optical properties of the powders. *Phys Chem* 2002;**4**:5683–9.
7. Carreto E, Montoya de la Fuente JA, Morgado J, Piña C, Cordoncillo E, Carda JB. Solid–solution formation in the synthesis of Fe–zircon. *J Am Ceram Soc* 2004;**87**:612–6.
8. Mosset A, Baules P, Lecante P, Trombe JC, Ahamdane H, Bensamka F. A new solution route to silicates. Part 4. Submicronic zircon powders. *J Mater Chem* 1996;**6**:1527–32.
9. Valentín C, Muñoz MC, Alarcón J. Synthesis and characterization of vanadium-containing $ZrSiO_4$ solid solutions from gels. *J Sol–Gel Sci Tech* 1999;**15**:221–30.

10. Ocaña M, Fórnes V, Serna CJ. The variability of the infrared spectrum of amorphous SiO_2. *J Non-Cryst Solids* 1989;**107**:187–92.
11. Ocaña M, Fórnes V, Serna CJ. A simple procedure for the preparation of spherical oxide particles by hydrolysis of aerosols. *Ceram Int* 1992;**18**:99–106.
12. Nogami M. Glass preparation of the ZrO_2–SiO_2 system by the sol–gel process from metal alkoxides. *J Non-Cryst Solids* 1985;**69**:415–23.
13. Valentín C, Sales M, Alarcón J. V-$ZrSiO_4$ solid solutions prepared from colloidal gels. Synthesis and characterization. *Bol Soc Esp Cerám Vidrio* 1998;**37**:39–46.
14. Pecharromán C, Ocaña M, Tartaj P, Sanz J, Serna CJ. Infrared optical properties of zircon. *Mater Res Bull* 1994;**29**:417–26.
15. Alarcón J. Crystallization behaviour and microstructural development in $ZrSiO_4$ and V–$ZrSiO_4$ solid solutions from colloidal gels. *J Eur Ceram Soc* 2000;**20**:1749–58.
16. Tartaj P, Sanz J, Serna CJ, Ocaña M. Zircon formation from amorphous spherical $ZrSiO_4$ particles obtained by hydrolysis of aerosols. *J Mater Sci* 1994;**29**:6533–8.
17. Ono T, Kagawa M, Syono Y. Ultrafine particles of the ZrO_2–SiO_2 system prepared by the spray-ICP technique. *J Mater Sci* 1985;**20**: 2483–7.
18. Kanno Y, Suzuki T. Effect of matrices on the phase transformation of ZrO_2 in the ZrO_2–MO_x ($MO_x = SiO_2$, Al_2O_3) system. *J Mater Sci Lett* 1989;**8**:41–3.
19. Garvie RC. The occurrence of metastable tetragonal zirconia as a crystallite size effect. *J Phys Chem* 1965;**69**:1238–43.
20. Shannon RD. Revised effective ionic radii and systematic studies of interatomic distances in halides and chalcogenides. *Acta Cryst A* 1976;**32**:751–67.